

World Journal of *Radiology*

World J Radiol 2023 March 28; 15(3): 56-88



REVIEW

- 56 Hepatocellular carcinoma: State of the art diagnostic imaging
Criss C, Nagar AM, Makary MS

MINIREVIEWS

- 69 Multi-modality parathyroid imaging: A shifting paradigm
Gulati S, Chumber S, Puri G, Spalkit S, Damle NA, Das CJ

CASE REPORT

- 83 Magnetic resonance imaging findings of spontaneous pyomyoma in a premenopausal woman managed with myomectomy: A case report
Martínez D, Sanchez GE, Gómez J, Sonda LJ, Suárez LD, López CS, Vega JJ, Cepeda DA

ABOUT COVER

Editorial Board Member of *World Journal of Radiology*, Wing-Chi E Kwok, PhD, Associate Professor, Department of Imaging Sciences, University of Rochester, Rochester, NY 14642, United States.
edmund_kwok@urmc.rochester.edu

AIMS AND SCOPE

The primary aim of *World Journal of Radiology (WJR, World J Radiol)* is to provide scholars and readers from various fields of radiology with a platform to publish high-quality basic and clinical research articles and communicate their research findings online.

WJR mainly publishes articles reporting research results and findings obtained in the field of radiology and covering a wide range of topics including state of the art information on cardiopulmonary imaging, gastrointestinal imaging, genitourinary imaging, musculoskeletal imaging, neuroradiology/head and neck imaging, nuclear medicine and molecular imaging, pediatric imaging, vascular and interventional radiology, and women's imaging.

INDEXING/ABSTRACTING

The *WJR* is now abstracted and indexed in PubMed, PubMed Central, Emerging Sources Citation Index (Web of Science), Reference Citation Analysis, China National Knowledge Infrastructure, China Science and Technology Journal Database, and Superstar Journals Database. The 2022 edition of Journal Citation Reports® cites the 2021 Journal Citation Indicator (JCI) for *WJR* as 0.48.

RESPONSIBLE EDITORS FOR THIS ISSUE

Production Editor: Xiang-Di Zhang; Production Department Director: Xu Guo; Editorial Office Director: Jia-Ru Fan.

NAME OF JOURNAL

World Journal of Radiology

ISSN

ISSN 1949-8470 (online)

LAUNCH DATE

January 31, 2009

FREQUENCY

Monthly

EDITORS-IN-CHIEF

Thomas J Vogl

EDITORIAL BOARD MEMBERS

<https://www.wjgnet.com/1949-8470/editorialboard.htm>

PUBLICATION DATE

March 28, 2023

COPYRIGHT

© 2023 Baishideng Publishing Group Inc

INSTRUCTIONS TO AUTHORS

<https://www.wjgnet.com/bpg/gerinfo/204>

GUIDELINES FOR ETHICS DOCUMENTS

<https://www.wjgnet.com/bpg/GerInfo/287>

GUIDELINES FOR NON-NATIVE SPEAKERS OF ENGLISH

<https://www.wjgnet.com/bpg/gerinfo/240>

PUBLICATION ETHICS

<https://www.wjgnet.com/bpg/GerInfo/288>

PUBLICATION MISCONDUCT

<https://www.wjgnet.com/bpg/gerinfo/208>

ARTICLE PROCESSING CHARGE

<https://www.wjgnet.com/bpg/gerinfo/242>

STEPS FOR SUBMITTING MANUSCRIPTS

<https://www.wjgnet.com/bpg/GerInfo/239>

ONLINE SUBMISSION

<https://www.f6publishing.com>

Multi-modality parathyroid imaging: A shifting paradigm

Shrea Gulati, Sunil Chumber, Gopal Puri, Stanzin Spalkit, N A Damle, CJ Das

Specialty type: Radiology, nuclear medicine and medical imaging

Provenance and peer review: Invited article; Externally peer reviewed.

Peer-review model: Single blind

Peer-review report's scientific quality classification

Grade A (Excellent): 0
Grade B (Very good): 0
Grade C (Good): C, C
Grade D (Fair): 0
Grade E (Poor): 0

P-Reviewer: Nambi G, Saudi Arabia; Wu SZ, China

Received: December 24, 2022

Peer-review started: December 24, 2022

First decision: January 3, 2023

Revised: January 20, 2023

Accepted: March 1, 2023

Article in press: March 1, 2023

Published online: March 28, 2023



Shrea Gulati, Stanzin Spalkit, CJ Das, Department of Radiodiagnosis and Interventional Radiology, All India Institute of Medical Sciences, New Delhi 110029, Delhi, India

Sunil Chumber, Gopal Puri, Department of Surgical Disciplines, All India Institute of Medical Sciences, New Delhi 110029, Delhi, India

N A Damle, Department of Nuclear Medicine, All India Institute of Medical Sciences, New Delhi 110029, Delhi, India

Corresponding author: CJ Das, FRCP, MBBS, MD, Professor, Department of Radiodiagnosis and Interventional Radiology, All India Institute of Medical Sciences, Aurobindo Marg Ansari Nagar, New Delhi 110029, Delhi, India. docchandan17@gmail.com

Abstract

The goal of parathyroid imaging in hyperparathyroidism is not diagnosis, rather it is the localization of the cause of hyperparathyroidism for planning the best therapeutic approach. Hence, the role of imaging to accurately and precisely localize the abnormal parathyroid tissue is more important than ever to facilitate minimally invasive parathyroidectomy over bilateral neck exploration. The common causes include solitary parathyroid adenoma, multiple parathyroid adenomas, parathyroid hyperplasia and parathyroid carcinoma. It is highly imperative for the radiologist to be cautious of the mimics of parathyroid lesions like thyroid nodules and lymph nodes and be able to differentiate them on imaging. The various imaging modalities available include high resolution ultrasound of the neck, nuclear imaging studies, four-dimensional computed tomography (4D CT) and magnetic resonance imaging. Contrast enhanced ultrasound is a novel technique which has been recently added to the armamentarium to differentiate between parathyroid adenomas and its mimics. Through this review article we wish to review the imaging features of parathyroid lesions on various imaging modalities and present an algorithm to guide their radiological differentiation from mimics.

Key Words: Parathyroid adenoma; Ultrasound; Four-dimensional computed tomography; Magnetic resonance imaging; Nuclear Imaging; Contrast enhanced ultrasound

©The Author(s) 2023. Published by Baishideng Publishing Group Inc. All rights reserved.

Core Tip: Parathyroid adenoma is the commonest cause of primary hyperparathyroidism, the management of which lies in definitive surgery. Accurate preoperative imaging is of prime importance to facilitate surgery. Imaging modalities include radiological investigations like ultrasound, four-dimensional computed tomography and magnetic resonance imaging which provide anatomical localization and nuclear scans like MIBI, single photon emission computed tomography and Fluoro-choline positron emission tomography which provide functional imaging details. Contrast-enhanced ultrasound is a novel modality which is being explored in the evaluation of parathyroid adenomas.

Citation: Gulati S, Chumber S, Puri G, Spalkit S, Damle NA, Das CJ. Multi-modality parathyroid imaging: A shifting paradigm. *World J Radiol* 2023; 15(3): 69-82

URL: <https://www.wjgnet.com/1949-8470/full/v15/i3/69.htm>

DOI: <https://dx.doi.org/10.4329/wjr.v15.i3.69>

INTRODUCTION

Primary hyperparathyroidism is the commonest cause of hypercalcemia resulting from pathologies intrinsic to the parathyroid glands[1]. It manifests biochemically as raised parathyroid hormone and calcium levels[2]. Primary hyperparathyroidism is most commonly due to a single benign parathyroid adenoma (approximately 80% of the patients), with multiglandular disease seen in approximately 15%-20% of patients[3]. Primary hyperparathyroidism is due to multiglandular involvement consisting of either multiple adenomas or hyperplasia of all 4 glands (5%-10%) and very rarely by parathyroid carcinoma (< 1%)[4]. The definitive management is achieved by surgical excision of the abnormal parathyroid tissue. Preoperative imaging is mandatory in deciding the surgical approach and improves localisation of the abnormal gland. The commonly accepted modalities to guide imaging include ultrasound, 4-dimensional computed tomography (4D CT), magnetic resonance imaging (MRI) and nuclear medicine studies whereas contrast-enhanced ultrasound (CEUS) is the new kid on the block. In this review, we would like to revisit the characteristic imaging findings on various modalities and will present an algorithm of differentiating parathyroid adenomas from their mimics.

ANATOMY

The usual number of parathyroid glands is four, but this can vary. Some persons have more than four parathyroid glands. The normal shape of the parathyroid gland is ovoid or bean shaped and it measures 4-6 mm in length, 2-4 mm in width and 1-2 mm in thickness. The plane of the recurrent laryngeal nerve (RLN), identified by the trachea-oesophageal groove helps identify the superior and inferior parathyroid glands, the superior is posterior to the RLN while the inferior is anterior to the RLN[5]. In 16 % of the individuals the parathyroid glands are ectopically located[6]. The embryological origin of the inferior parathyroid glands is from the third pharyngeal pouch while the origin of the superior parathyroid gland is from the fourth pharyngeal pouch. The longer course of embryological migration of the superior parathyroid glands makes it more prone for ectopic location. Ectopic superior parathyroid glands are found in the retropharyngeal or retroesophageal locations, while ectopic inferior parathyroid glands may be seen within the carotid sheath or mediastinum (Figure 1)[7]. Uncommonly, there may be failure of descent of the inferior parathyroid glands, which may be finally located cephalad to the superior parathyroid glands[8].

ROLE OF IMAGING

The diagnosis of primary hyperparathyroidism is made biochemically with demonstration of raised parathormone (PTH) levels. The role of radiology in hyperparathyroidism is not diagnosis, rather it is accurate localisation and surgical planning[5]. There are two approaches to surgical management of hyperparathyroidism - bilateral neck exploration (BNE) and minimally invasive parathyroidectomy (MIP). BNE is the conventional surgical approach which involves a large midline surgical incision, exploration and examination of all four parathyroid glands and excision of the abnormal tissue. Due to the large incision involved and meticulous exploration, it is associated with excellent long term cure rates[9]. The downside of this meticulousness is the associated higher risk of recurrent laryngeal nerve damage and poor cosmesis. MIP involves a unilateral small incision on the affected side and surgical removal of only the pathological gland identified precisely and accurately by preoperative imaging studies[5]. As per the European Society of Endocrine Surgeons, in experienced hands, keeping in view

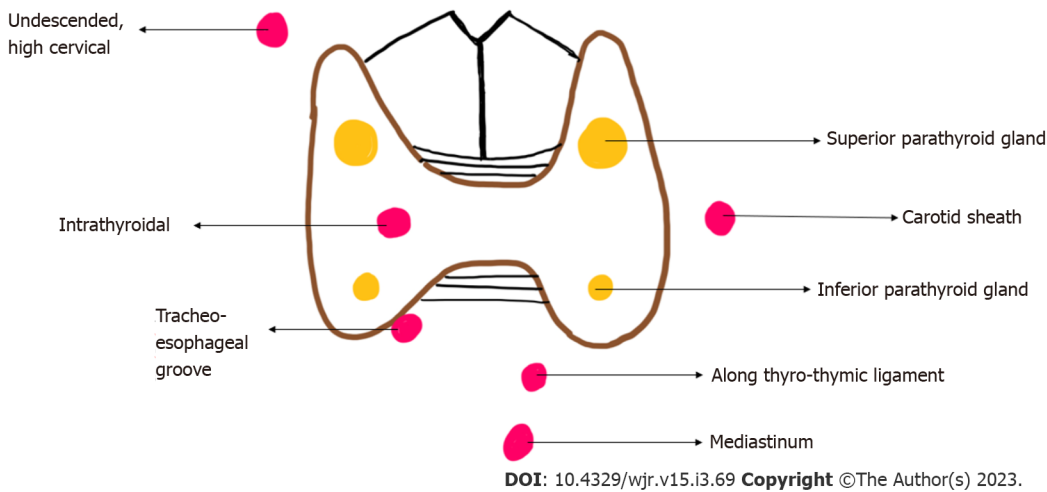


Figure 1 Diagrammatic representation of location of eutopic (yellow) and ectopic (red) parathyroid glands.

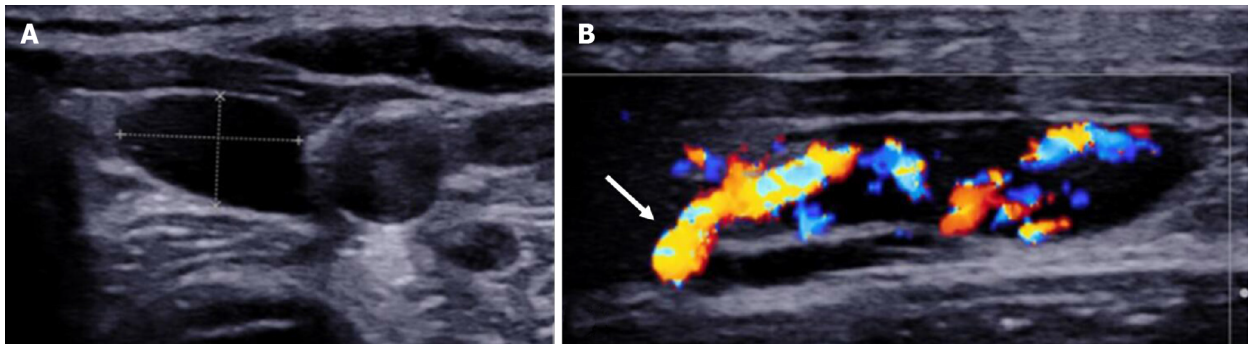


Figure 2 Left inferior parathyroid adenoma. A: High resolution ultrasound image of the neck in the transverse plane demonstrates a well-circumscribed homogeneously hypoechoic ovoid lesion located at the lower pole of the left lobe of thyroid gland; B: Colour Doppler shows a big feeding vessel, likely from the inferior thyroid artery (arrow) supplying the lesion.

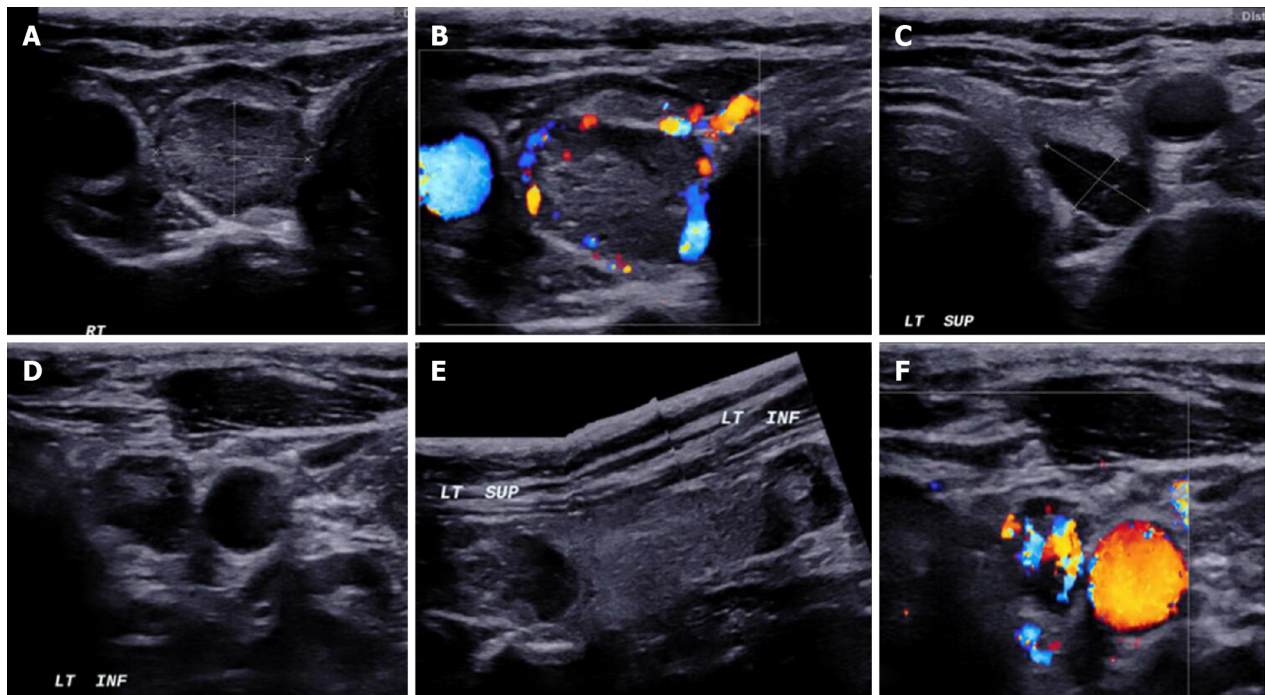
the indications and contraindications of the surgery, MIP is a reliable and safe procedure with equivalent cure rates[9]. As compared to BNE, MIP is associated with shorter operative times, better cosmesis, shorter hospital stays and therefore lower costs[10].

IMAGING

The imaging techniques available for parathyroid imaging include high resolution ultrasound of the neck, Tc99m sestamibi scan, 4D CT and MRI.

HIGH RESOLUTION ULTRASONOGRAPHY

Duplex ultrasound with a linear array transducer with 10 MHz or higher frequency is used for imaging of the parathyroid glands. With the patient in supine position and mild neck extension (using a pillow under the upper back), the neck is scanned in both transverse and longitudinal planes focusing on the region behind the thyroid gland. The normal location of parathyroid glands lesions is lateral to the trachea and oesophagus and medial to the carotid artery and the jugular vein. This knowledge helps to closely inspect the expected locations meanwhile differentiating it from close mimics. The small size and deep location of the normal parathyroid gland makes it non-identifiable on ultrasound. Parathyroid adenomas which are larger than 1 cm in size are readily visible on ultrasound. The sonographic detection of small parathyroid adenomas, especially those < 1 cm in size can be enhanced by using graded compression technique[11]. Parathyroid adenomas are oval/bean shaped, well circumscribed lesions which are homogeneously hypoechoic as compared to the neighbouring thyroid gland (Figure 2). Color Doppler provides associate information of the origin and course of the feeding artery of the



DOI: 10.4329/wjr.v15.i3.69 Copyright ©The Author(s) 2023.

Figure 3 In a patient with MEN-1 syndrome. A-F: Ultrasound neck images show multiple (3) parathyroid adenoma in the right superior and left superior and inferior parathyroid glands respectively.

parathyroid adenoma[12,13]. This is attributed to the high vascularity of the parathyroid adenomas which are supplied by an enlarged feeding inferior thyroidal artery (Feeding vessel sign). Spectral Doppler can determine the blood flow velocity of the feeding artery and get information of a low resistive index. This polar vascularity sign helps in differentiation from a lymph node which typically shows central hilar vascularity on Doppler[14]. Along with hypervascularity of the affected parathyroid, the ipsilateral thyroid gland can also show hyperaemia in 85% of the cases and this may serve as a surrogate marker of underlying parathyroid adenoma[11,14]. In patients with known syndromes like MEN-1 (Figure 3), multiple adenomas can be seen and identification of a single adenoma should not lead to a false sense of satisfaction of search. Uncommonly, parathyroid adenomas can show atypical features such as ectopic location, completely intrathyroidal location, internal areas of cystic degeneration, heterogenous internal echotexture rather than the homogenous hypoechoic echotexture which make prospective sonographic diagnosis difficult[15-18].

High resolution ultrasound has the advantage of non-involvement of radiation, low cost and easy availability. Although ultrasound is highly operator dependant in the detection of parathyroid adenomas, it has a sensitivity of 84% in the hands of an experienced sonologist[19]. The two most important differentials of parathyroid adenomas are thyroid nodules and lymph nodes, and ultrasound is a useful modality for their differentiation (Table 1). The oesophagus and the longus colli muscle can sometimes mimic parathyroid adenomas[14].

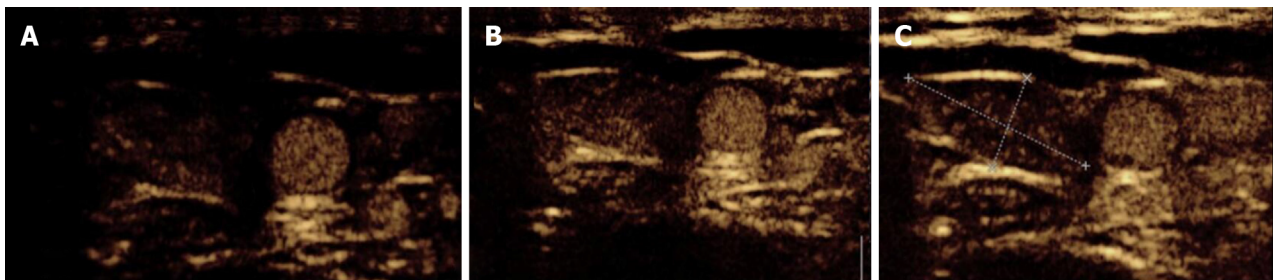
CEUS

CEUS is the new armamentarium added in the evaluation of parathyroid adenomas. The differentiation of parathyroid adenomas from parathyroid hyperplasia as well as non-parathyroid lesions like lymph nodes and thyroid nodules is difficult on conventional ultrasound[7,20]. Studies have demonstrated the use of contrast enhanced ultrasound as a novel technique in the differentiation of these entities[21-23]. On CEUS, parathyroid adenomas show early peripheral hyperenhancement with central washout in the later phases (Figure 4)[21]. Parathyroid hyperplasia on the other hand shows more homogenous contrast uptake[21]. Physiological lymph nodes show homogenous and centrifugal pattern of enhancement[24-26]. Thyroid nodules tend to show homogenous hyperenhancement with a fast wash-in and slow washout pattern[21].

Table 1 Differentiating features of parathyroid adenoma from lymph nodes and thyroid nodules on imaging

Modality	Features	Parathyroid adenoma	Thyroid nodule	Lymph node
USG	Echogenicity	Homogenously markedly hypoechoic	Homo/Heterogenously hypo/isoechoic	Central echogenic hilum
	Vascularity	Peripheral polar vessel sign present	Not seen	Central/hilar vascularity
	Calcification	Less common	Common	+/-
	Cystic changes	Less common	More common	+/-
CT	Non contrast	Hypodense	Hyperdense	Hypodense
	Arterial	Intense arterial enhancement	Enhancement in arterial phase but less than parathyroid adenomas	No enhancement in the arterial phase
	Venous	Washout	Persistent enhancement	Progressive enhancement in venous phase
MRI	Morphology	Cleavage plane with thyroid gland	No cleavage plane	Cleavage plane present
	Diffusion weighted Image	High SI		High SI
PET Choline	Uptake	Present	Variable	Uptake may be present, however is delayed and of lesser intensity

USG: Ultrasound; CT: Computed tomography; MRI: Magnetic resonance imaging; SI: Signal intensity; PET: Positron emission tomography.



DOI: 10.4329/wjr.v15.i3.69 Copyright ©The Author(s) 2023.

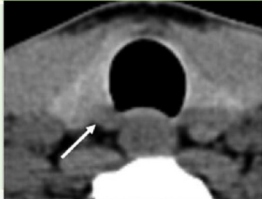
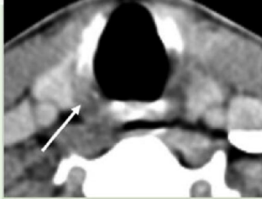
Figure 4 Contrast-enhanced ultrasound in parathyroid adenoma. A-C: A 33-year-old female with raised parathormone levels (87 IU) was assessed using contrast enhanced ultrasound. A circumscribed lesion at the lower pole of the left lobe of thyroid gland was found consistent with parathyroid adenoma, demonstrating early peripheral enhancement with central washout.

SHEAR WAVE ELASTOGRAPHY

This is a newer modality which has been explored for distinguishing parathyroid adenoma from the neighbouring thyroid tissue. Parathyroid adenomas show a significantly lower tissue elasticity than thyroid tissue. This may serve as an additional differentiating feature between the two entities[27].

PARATHYROID SCINTIGRAPHY

The most common radiotracer used for imaging parathyroid glands is sestamibi with ^{99m}Tc . Both thyroid and parathyroid glands take up sestamibi, however the differentiating point is that the uptake by hyperplastic or adenomatous parathyroid tissue is more intense, and also shows a delayed wash-out as compared to thyroid tissue which shows faster wash-out[28]. Therefore, foci of increased radiotracer uptake persisting on a delayed scan (variably acquired at 60-180 min after radio-tracer administration) represents parathyroid tissue. Subtracting images acquired by using two radio-tracer agents, the first one which is taken up by both thyroid and parathyroid tissue (like sestamibi) and a second which is taken up by only thyroid tissue (^{99m}Tc pertechnetate or ^{123}I) can help image the parathyroid. This was the basis of the famous Thallium- Technetium subtraction scan. However, this technique is less used these days due to the availability of more effective radiotracer, sestamibi.

S no.	Phase of CT	Region scanned	Time delay after start of contrast injection	Imaging features	Representative image
1	Non-contrast	Hyoid bone to clavicle	-	Hypodense (as compared to the thyroid gland which is hyperdense)	
2	Arterial phase	Angle of mandible to carina	25 s	Hyperenhancement on the arterial phase	
3	Delayed (venous phase)	Angle of mandible to carina	80 s	Washout on the venous phase	

DOI: 10.4329/wjr.v15.i3.69 Copyright ©The Author(s) 2023.

Figure 5 Imaging features of parathyroid adenomas on four-dimensional computed tomography. CT: Computed tomography.

4D CT

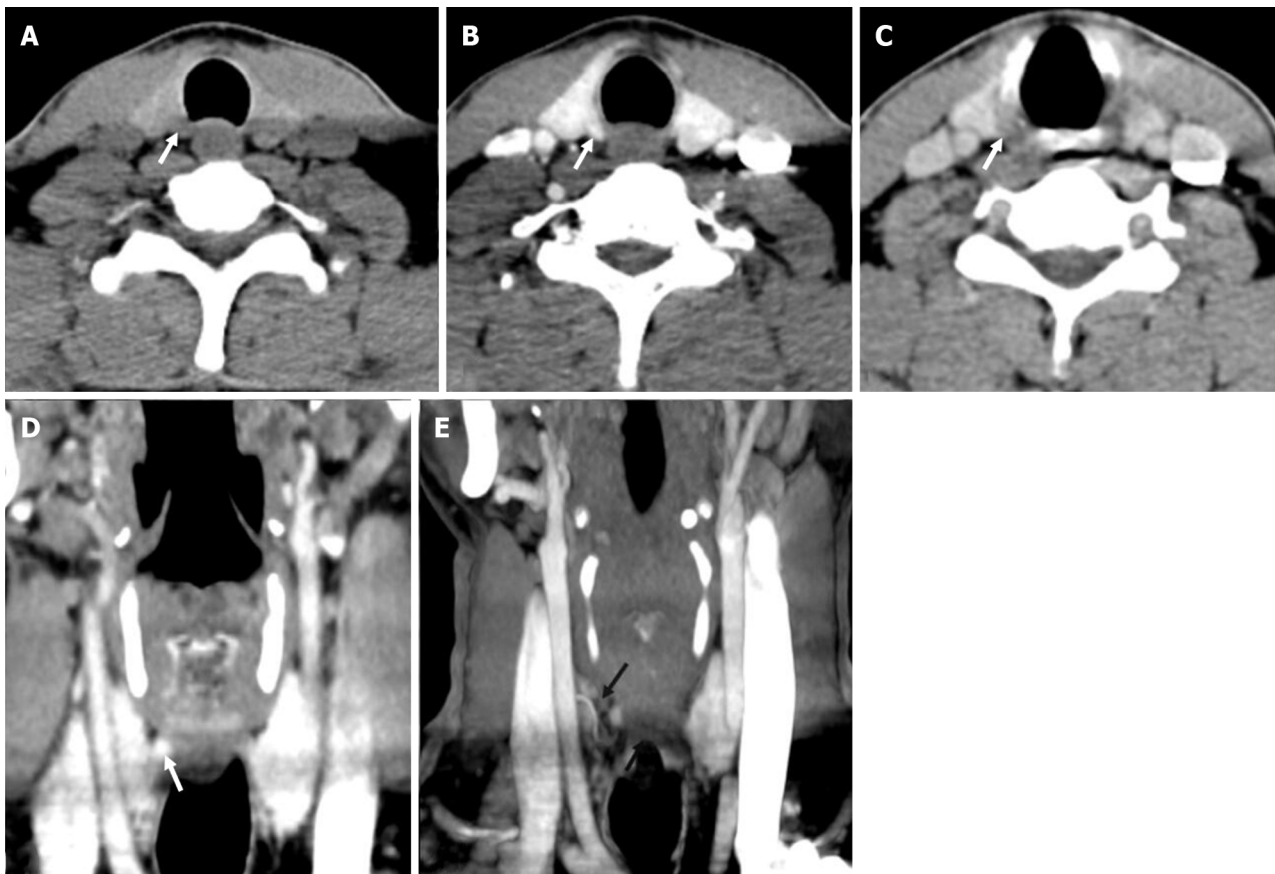
4D CT is advantageous over both ultrasonography and nuclear imaging studies in the precise localisation of both orthotopic and ectopic glands and better differentiation of parathyroid adenomas from mimics like lymph nodes and thyroid nodules (Table 1)[29]. 4D-CT demonstrates an accuracy of 93%. 4D-CT has a suboptimal 44% sensitivity, but 100% specificity, for multigland disease[30].

The first three dimensions in 4D CT are the three planes of image interpretation - axial, sagittal and coronal, while the fourth dimension refers to the change in enhancement pattern with time in the non-contrast, arterial and delayed (venous) phases (Figure 5).

Streak artifacts from hyperattenuating materials like high density contrast in neck vessels and surgical clips can hamper evaluation. The streak artifact caused by venous pooling may be prevented by using a saline chase after contrast injection[29]. The beam hardening artifact caused by clavicles and the shoulder girdle can interfere with interpretation of imaging findings which may be reduced by neck elevation achieved by putting a rolled towel under the shoulders[29]. In addition, patients are advised to avoid speaking, swallowing or coughing during image acquisition to avoid motion artifacts.

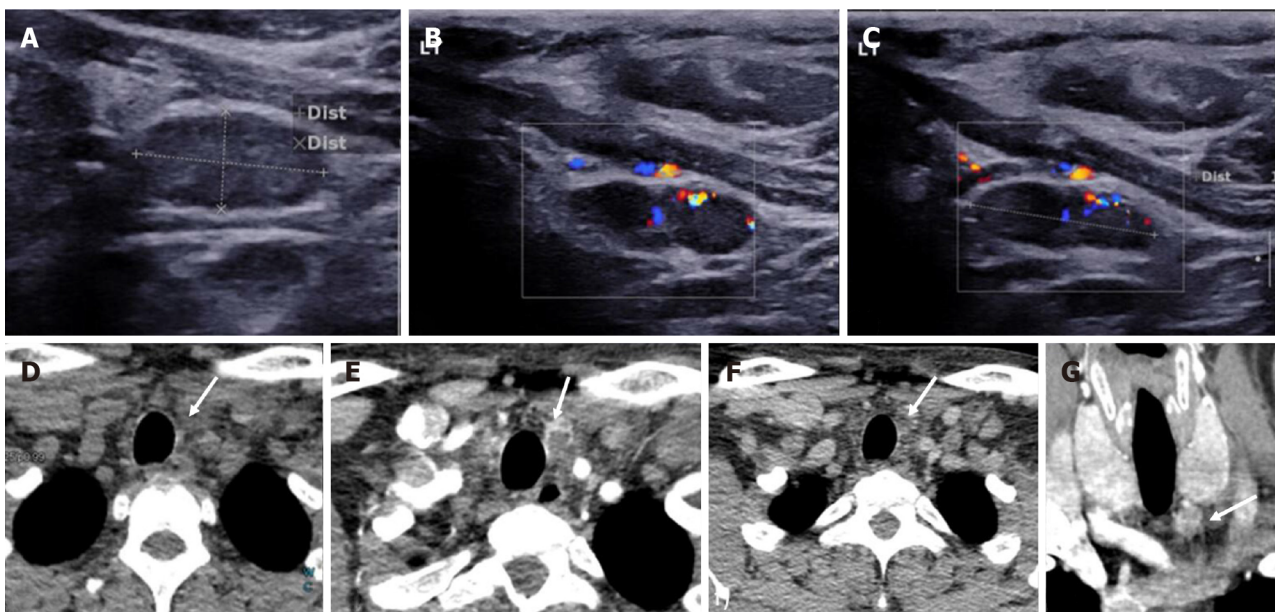
In order to facilitate the precise detection of parathyroid adenomas, Hoang *et al*[29] described a systematic five step approach: (1) Search for potential ectopic lesions in the arterial phase (2) Search for potential ectopic lesions in the arterial phase (3) Review the pattern of enhancement on other phases (4) Evaluate the morphological appearance; and (5) Correlate the computed tomography (CT) findings with other imaging modalities and clinical history. The characteristic imaging findings of a parathyroid adenoma are low attenuation on the non-contrast image, intense arterial enhancement (138-180 HU) and wash-out in the venous phase (Figures 6 and 7)[31,32]. The low attenuation on non-contrast images is important to differentiate from thyroid lesions, which are hyperdense on non-contrast CT owing to the iodine content. The typical search should start from the most common location of parathyroid adenoma *i.e.*, around the thyroid gland. This should be followed by a keen search along the expected path of migration of parathyroid glands *i.e.*, superiorly extending from the level of carotid bifurcation to the carina inferiorly. Rarer sites of ectopic parathyroid adenomas like the retropharyngeal space and intrathyroidal locations should also be screened (Figures 8-11).

Since the ultimate goal of imaging is to facilitate precise operative planning, it is important to provide the surgeon with relevant information while reporting parathyroid adenomas preferably using a predefined cartoon (Figure 1). This includes number of candidate lesions, size of the lesions, location of the lesion with respect to standard surgical landmarks (superior and inferior thyroid poles, suprasternal notch and trachea-oesophageal groove), ectopic or supernumerary parathyroid glands, underlying thyroid pathology and arterial anomalies associated with non-recurrent laryngeal nerve (aberrant right subclavian artery) which may increase risk of operative injury to the nerve[5].



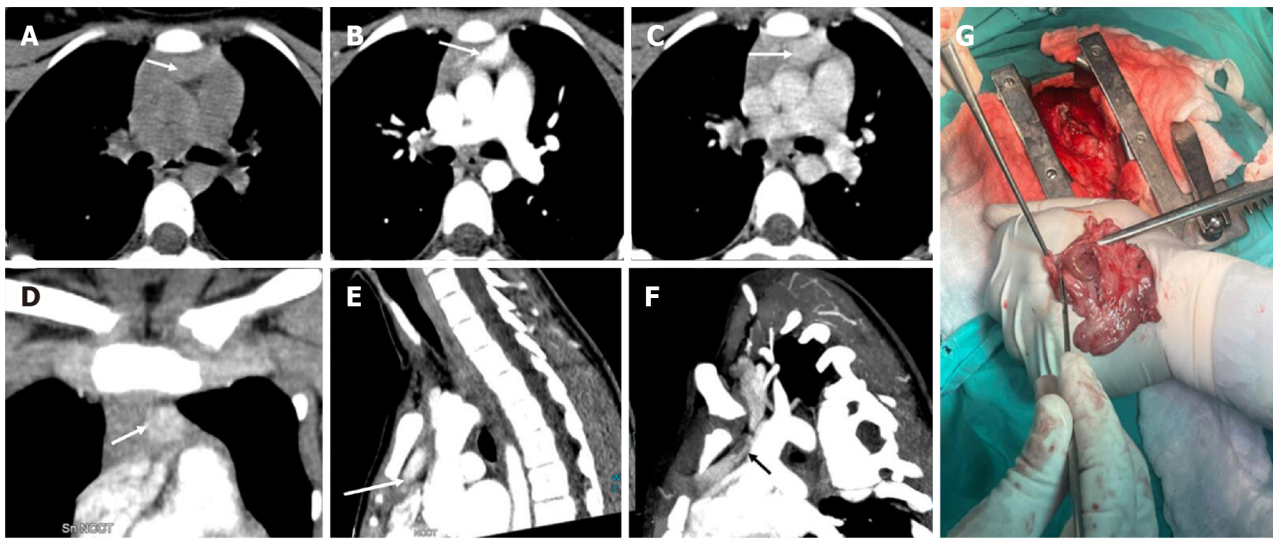
DOI: 10.4329/wjr.v15.i3.69 Copyright ©The Author(s) 2023.

Figure 6 Right superior adenoma: Four-dimensional computed tomography. A: Non-contrast computed tomography shows a small oval hypodense lesion which shows B: Intense enhancement on the arterial phase; C: Washout on the venous phase consistent with right superior parathyroid adenoma; D: Coronal image and E: Coronal maximum intensity projection image in the arterial phase better demonstrate the lesion with the feeding vessel (black arrow).



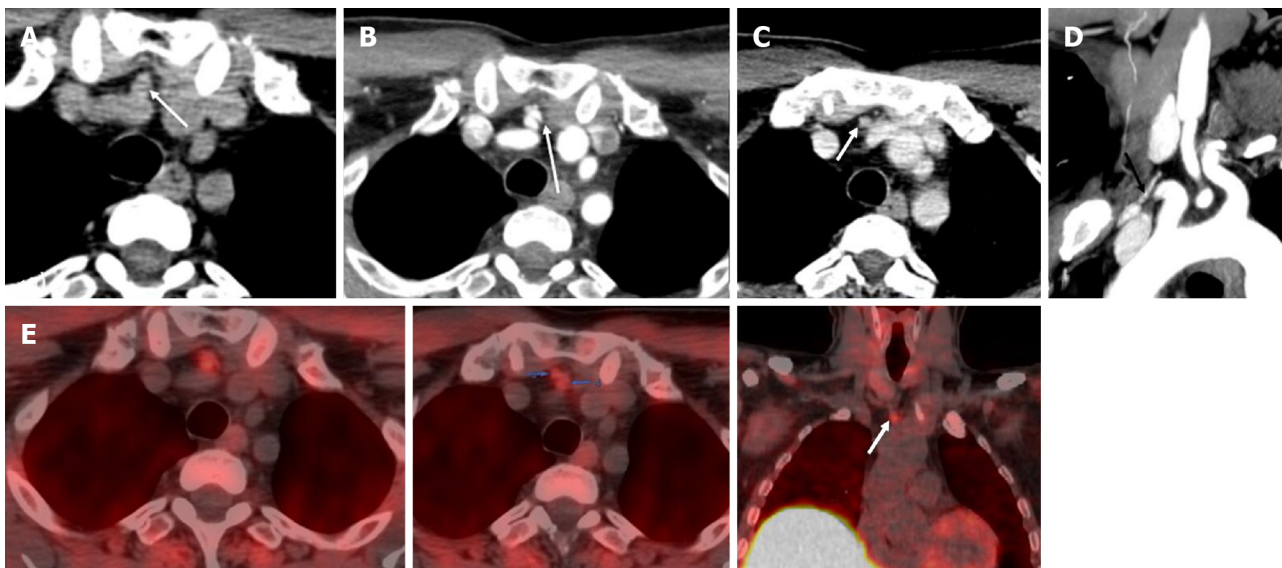
DOI: 10.4329/wjr.v15.i3.69 Copyright ©The Author(s) 2023.

Figure 7 Left inferior parathyroid adenoma. In a patient with raised parathormone levels (290 IU), grey scale ultrasound A: and colour doppler flow imaging; B and C: Showed a hypoechoic lesion with vascularity just below the left lobe of the; D: 4-dimensional computed tomography showed the lesion to be hypodense on noncontrast computer tomography; E: Hyperenhancing with central necrosis on arterial phase; F: Washout on the venous phase; G: Coronal image better demonstrates the lesion.



DOI: 10.4329/wjr.v15.i3.69 Copyright ©The Author(s) 2023.

Figure 8 Ectopic parathyroid adenoma in the anterior mediastinum. A: 4-dimensional computed tomography done in the 12-year-old female with hyperparathyroidism showed a well-defined lesion in the anterior mediastinum just behind the sternum which was hypodense on non-contrast computed tomography; B: intense arterial enhancement; C: washout on the venous phase; D: Multiplanar reformatted coronal; E: sagittal images in the arterial phase show the lesion better; F: Oblique sagittal maximum intensity projection image shows the feeding vessel (black arrow); G: Sternotomy followed by thymectomy was done and the thymus opened - the adenoma can be seen within the thymic parenchyma as pointed by the forceps.

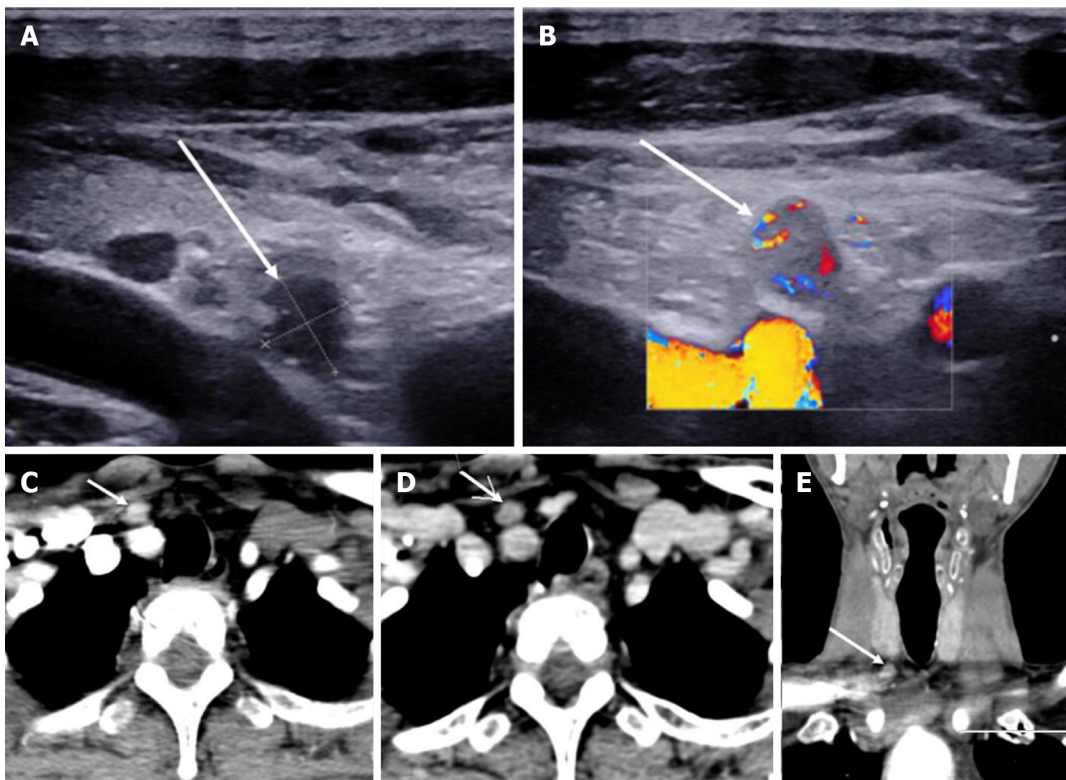


DOI: 10.4329/wjr.v15.i3.69 Copyright ©The Author(s) 2023.

Figure 9 Ectopic parathyroid adenoma in the anterior mediastinum. A: Computed tomography in a 45-year-old male patient showed a well-defined ovoid lesion in the prevascular space just posterior to the sternal notch and anterior to the inferior thyroid vessels appearing hypodense on the non-contrast phase; B: Showing intense enhancement on the arterial phase; C: washout in the venous phase; D: Coronal maximum intensity projection image demonstrates the inferior thyroid artery supplying the lesion (feeding vessel - black arrows); E: Fluoro-choline positron emission tomography shows a small tracer avid lesion in ectopic location which correlates with the computed tomography images.

Exophytic thyroid nodules and level VI cervical lymph nodes can mimic parathyroid adenomas as they have similar shape and locations. The differentiation may be done on the basis of contrast enhancement patterns. Thyroid nodules show high attenuation on the non-contrast image owing to their high iodine content and show delayed enhancement as compared to parathyroid adenoma. Lymph nodes although similar in shape to parathyroid adenomas can be differentiated from the latter based on contrast kinetics. Lymph nodes show progressive enhancement on the delayed phase as compared to parathyroid adenomas which show washout of contrast.

The detection of one lesion should not give a false sense of satisfaction to the radiologist since multiglandular disease can occur in 10% of the cases[33]. Hence, a relook is always suggested.



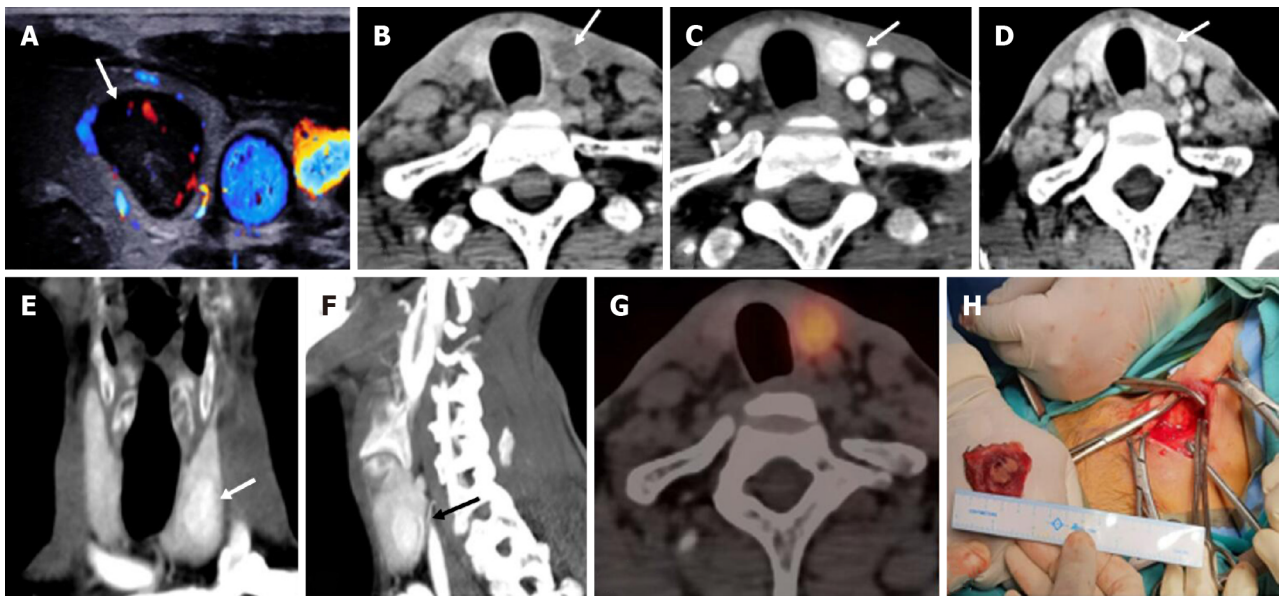
DOI: 10.4329/wjr.v15.i3.69 Copyright ©The Author(s) 2023.

Figure 10 Ectopic Parathyroid Adenoma in the Supraclavicular fossa. A: Grey scale ultrasound of the neck on a 49-year-old male patient, with history of bilateral renal stones and elevated parathormone reveals a hypoechoic lesion in the right supraclavicular location; B: On color doppler, internal vascularity was detected; C: 4-dimensional computed tomography showed a lesion with arterial enhancement; D: Washout seen on the venous phase; E: Coronal reformatted image better depicts the ectopic parathyroid adenoma in the right supraclavicular fossa.

While 4D CT is an excellent modality for detection of parathyroid adenomas, it does involve considerable radiation exposure. The effective dose is 10.4 mSv for 4D CT as compared to 7.8 mSv for nuclear scintigraphy, however 4D CT is associated with 50 times higher organ dose to the thyroid gland which becomes a cause of concern in young females since it increases the life time risk of development of thyroid cancer[34].

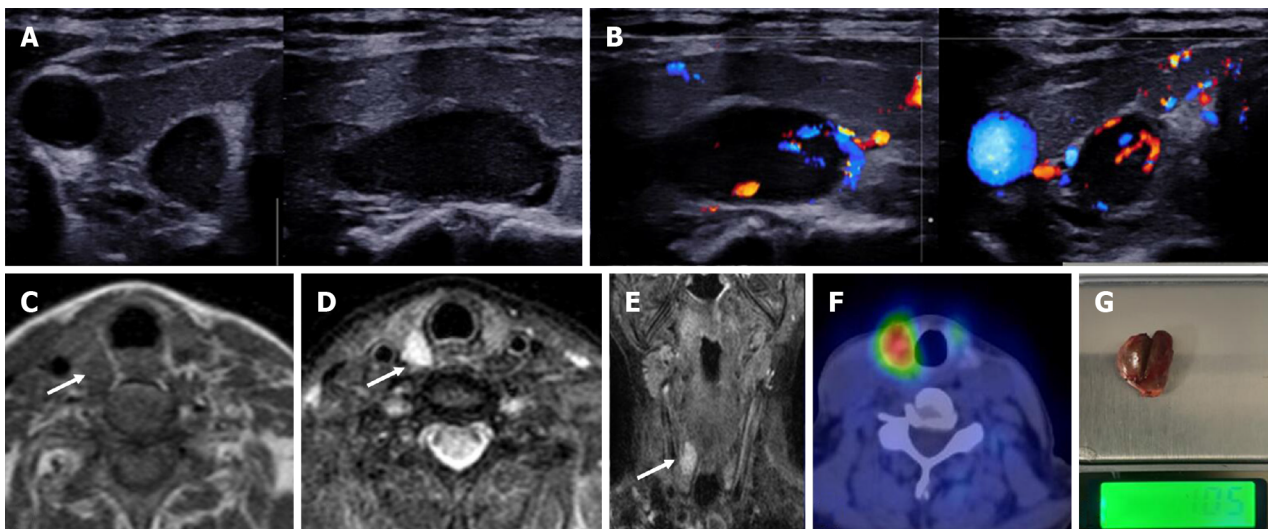
MRI

MRI is often not used as a first line modality. It is more commonly used as problem solving modality in patients with recurrent or residual disease. The non-involvement of ionizing radiation makes it a safer modality as compared to 4D CT and nuclear imaging studies; however, the modality is time consuming and isn't readily available. On a 1.5 T MRI machine, the sensitivity is 80% [35-37]. Benign parathyroid lesions are seen as well-circumscribed ovoid lesions with a cleavage plane with the thyroid tissue which is best seen on out of phase images[37]. The signal characteristics of parathyroid adenomas vary on MRI, but most commonly they tend to show homogenously hyperintense signal on T2 weighted images (Figure 12)[37]. Post gadolinium injection, they show rapid enhancement in the arterial phase. Solid parathyroid lesions show higher signal on diffusion weighted images as compared to the other anatomically neighbouring structures in the neck thus helping in differentiation from the former[38]. 4D MRI is a novel method which has been explored in the imaging of parathyroid adenomas. The sensitivity of 4D MRI was 90% and after optimisation, 100% and the specificity was 90% [39]. 4D MRI has similar accuracy to 4D CT for the detection of parathyroid lesions. However, 4D MRI has the advantage of lack of exposure to ionizing radiation, which can be beneficial in younger patients[40]. The protocol used is the acquisition of fast T1 VIBE sequences in the axial plane prior to and after administration of gadolinium acquiring the images every 13 s for 10 sequential scans[39]. Parathyroid adenomas showed fast enhancement after 26-30 s similar to their pattern on 4D CT[39].



DOI: 10.4329/wjr.v15.i3.69 Copyright ©The Author(s) 2023.

Figure 11 Intrathyroidal parathyroid adenoma. In a patient with raised parathormone (208 IU), A: Color doppler ultrasound of the neck showed a circumscribed solid hypoechoic lesion within the left lobe of thyroid gland; B: 4-dimensional computed tomography revealed the lesion to be hypodense as compared to thyroid tissue on non-contrast; C: showed intense arterial hyperenhancement; D: Washout on the venous phase, consistent with the diagnosis of intra-thyroid parathyroid adenoma; E and F: Coronal (E) and Sagittal maximum intensity projection images better depict the lesions with vascular pedicle (black arrow) seen supplying the lesion (F); G: Single photon emission computed tomography image showing a thyroid nodule which is mildly tracer avid; H: Left hemithyroidectomy was done and the cut open section confirmed the presence of the tumor.



DOI: 10.4329/wjr.v15.i3.69 Copyright ©The Author(s) 2023.

Figure 12 Right superior parathyroid adenoma. A 50-year-old female with raised parathormone levels (96 IU) was examined using duplex ultrasound for parathyroid glands. A: Grey scale sonography in the transverse and longitudinal plane showed a well circumscribed lesion posterior to the right lobe of thyroid gland and separated from it by a clear fat plane; B: Colour doppler image shows a feeding vessel. Corroborative magnetic resonance imaging axial images show a subcentimetric lesion (arrows) posterior to the middle third of the right lobe of thyroid gland which is C: T1 hypointense; D: T2 hyperintense; E: Coronal T2w image better demonstrates the lesion; F: Correlative single photon emission computed tomography component of MIBI scan showing tracer avid lesion at the superior pole of the right lobe of thyroid; G: Image of the resected adenoma weighing 1.05 g.

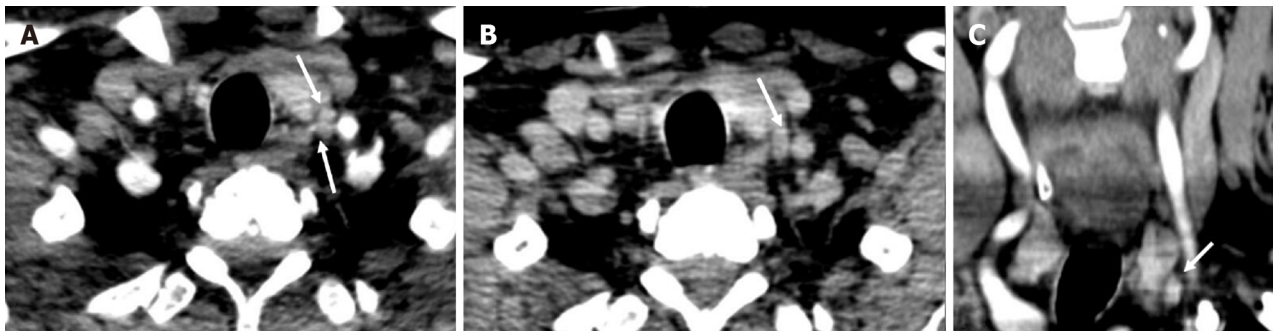
CHOLINE POSITRON EMISSION TOMOGRAPHY

Positron emission tomography (PET) is a non-invasive nuclear imaging study which provides both anatomical and functional information post intravenous injection of a radio-tracer agent. Choline labelled with positron emitters like carbon-11 or fluorine-18 is used for parathyroid imaging[41]. Increased choline uptake can be seen in parathyroid adenomas owing to the parathormone induced upregulation of choline kinase[42]. The image acquisition is done with the patient in a supine position

Table 2 Differentiating features of various parathyroid lesions

	Parathyroid hyperplasia	Parathyroid adenoma	Parathyroid carcinoma
USG	Small; Ovoid; Well-circumscribed; Homogeneously hypoechoic; Calcifications uncommon; No local invasion; CEUS - Homogeneous enhancement	Small; Ovoid; Well-circumscribed; Homogeneously hypoechoic; Calcifications uncommon; No local invasion; CEUS - Peripheral enhancement with central washout on delayed image	Large; Irregular shape; Non circumscribed margins; Heterogenous echotexture; Intra-nodular calcifications; Local invasion
CT	Small hypodense lesion (as compared to thyroid gland); Intense arterial enhancement; Washout on the venous phase; May not be identifiable on CT	Small hypodense lesion (as compared to thyroid gland); Intense arterial enhancement; Washout on the venous phase	Lesions may show infiltration into the surrounding structures
MRI	Small sized; Well defined; Homogenous; Low on T1; High on T2; Avid enhancement	Small sized; Well defined; Homogenous; Low on T1; High on T2; Avid enhancement	Large; Ill-defined; Heterogenous

USG: Ultrasound; CT: Computed tomography; MRI: Magnetic resonance imaging; CEUS: Contrast enhanced ultrasound.



DOI: 10.4329/wjr.v15.i3.69 Copyright ©The Author(s) 2023.

Figure 13 Parathyroid carcinoma. A 62-year-old male patient with recurrent hyperparathyroidism (previously operated parathyroid carcinoma), 4-dimensional computed tomography done showed few hypodense lesions with ill-defined margins near the lower pole of the left lobe of thyroid gland which showed, A: arterial enhancement however; B: No washout on the venous phase - atypical contrast kinetics for parathyroid adenoma; C: Coronal image better demonstrates the lesion. Surgical exploration and histopathological examination revealed parathyroid carcinoma recurrence.

about 45 to 60 min post intravenous injection of 18-fluoro choline[43]. Eyeballing is used to detect lesions in the eutopic or ectopic locations with parathyroid tissue being identified as maximum standardized uptake value (SUV max) four times greater than thyroid tissue[44]. Fluoro-choline PET can identify abnormal parathyroid gland in 92% patients in whom ultrasound and other nuclear imaging studies are negative[45]. It has excellent ability to detect small adenomas. The radiation dose is around 6 mSv which is lesser than that involved in MIBI scan and 4D CT. The scan involves a single acquisition as compared to the MIBI scan which involves imaging at two time points[46]. Choline is highly sensitive in the detection of parathyroid adenomas especially in multi-glandular disease. The high lesion to thyroid ratio improves the ability to detect smaller lesions. There are however several limitations with choline PET which include limited availability, high cost and the absence of a standardized protocol for imaging.

CONCLUSION

The primary goal of imaging in a clinically diagnosed case of hyperparathyroidism is precise localisation of the presence of parathyroid lesions which permits accurate surgical planning. The first line imaging modalities are ultrasound of the neck and scintigraphy. The inability to localise on these modalities or discordant findings on these modalities necessitates the use of 4D CT, MRI or F-Choline PET. Novel modalities such as contrast enhanced ultrasound and shear wave elastography of the neck should be coming up in a big way as it is free of radiation as well as safe for the kidneys. The various imaging modalities may also be used to differentiate parathyroid hyperplasia, parathyroid adenoma and parathyroid carcinoma (Table 2, Figure 13), though this may not always be possible and histopathological examination is the gold standard.

FOOTNOTES

Author contributions: Gulati S, Das JC, Spalkit S wrote the paper; Chumber S and Puri G provided the surgical expertise; Damle N provided the nuclear medicine expertise. All authors were involved in careful editing of the final manuscript.

Conflict-of-interest statement: All the authors declare that they have no conflict of interest.

Open-Access: This article is an open-access article that was selected by an in-house editor and fully peer-reviewed by external reviewers. It is distributed in accordance with the Creative Commons Attribution NonCommercial (CC BY-NC 4.0) license, which permits others to distribute, remix, adapt, build upon this work non-commercially, and license their derivative works on different terms, provided the original work is properly cited and the use is non-commercial. See: <https://creativecommons.org/licenses/by-nc/4.0/>

Country/Territory of origin: India

ORCID number: CJ Das 0000-0001-6505-5940.

S-Editor: Liu JH

L-Editor: A

P-Editor: Liu JH

REFERENCES

- 1 Fraser WD. Hyperparathyroidism. *Lancet* 2009; **374**: 145-158 [PMID: 19595349 DOI: 10.1016/S0140-6736(09)60507-9]
- 2 Bunch PM, Kelly HR. Preoperative Imaging Techniques in Primary Hyperparathyroidism: A Review. *JAMA Otolaryngol Head Neck Surg* 2018; **144**: 929-937 [PMID: 30193297 DOI: 10.1001/jamaoto.2018.1671]
- 3 Bilezikian JP, Bandeira L, Khan A, Cusano NE. Hyperparathyroidism. *Lancet* 2018; **391**: 168-178 [PMID: 28923463 DOI: 10.1016/S0140-6736(17)31430-7]
- 4 Bilezikian JP, Cusano NE, Khan AA, Liu JM, Marcocci C, Bandeira F. Primary hyperparathyroidism. *Nat Rev Dis Primers* 2016; **2**: 16033 [PMID: 27194212 DOI: 10.1038/nrdp.2016.33]
- 5 Bunch PM, Randolph GW, Brooks JA, George V, Cannon J, Kelly HR. Parathyroid 4D CT: What the Surgeon Wants to Know. *Radiographics* 2020; **40**: 1383-1394 [PMID: 32678698 DOI: 10.1148/rg.2020190190]
- 6 Phitayakorn R, McHenry CR. Incidence and location of ectopic abnormal parathyroid glands. *Am J Surg* 2006; **191**: 418-423 [PMID: 16490559 DOI: 10.1016/j.amjsurg.2005.10.049]
- 7 Kuzminski SJ, Sosa JA, Hoang JK. Update in Parathyroid Imaging. *Magn Reson Imaging Clin N Am* 2018; **26**: 151-166 [PMID: 29128002 DOI: 10.1016/j.mric.2017.08.009]
- 8 Akerström G, Malmaeus J, Bergström R. Surgical anatomy of human parathyroid glands. *Surgery* 1984; **95**: 14-21 [PMID: 6691181]
- 9 Wilhelm SM, Wang TS, Ruan DT, Lee JA, Asa SL, Duh QY, Doherty GM, Herrera MF, Pasiacka JL, Perrier ND, Silverberg SJ, Solórzano CC, Sturgeon C, Tublin ME, Udelsman R, Carty SE. The American Association of Endocrine Surgeons Guidelines for Definitive Management of Primary Hyperparathyroidism. *JAMA Surg* 2016; **151**: 959-968 [PMID: 27532368 DOI: 10.1001/jamasurg.2016.2310]
- 10 Minisola S, Cipriani C, Diacinti D, Tartaglia F, Scillitani A, Pepe J, Scott-Coombes D. Imaging of the parathyroid glands in primary hyperparathyroidism. *Eur J Endocrinol* 2016; **174**: D1-D8 [PMID: 26340967 DOI: 10.1530/EJE-15-0565]
- 11 Reeder SB, Desser TS, Weigel RJ, Jeffrey RB. Sonography in primary hyperparathyroidism: review with emphasis on scanning technique. *J Ultrasound Med* 2002; **21**: 539-52; quiz 553 [PMID: 12008817 DOI: 10.7863/jum.2002.21.5.539]
- 12 Wolf RJ, Cronan JJ, Monchik JM. Color Doppler sonography: an adjunctive technique in assessment of parathyroid adenomas. *J Ultrasound Med* 1994; **13**: 303-308 [PMID: 7932996 DOI: 10.7863/jum.1994.13.4.303]
- 13 Lane MJ, Desser TS, Weigel RJ, Jeffrey RB Jr. Use of color and power Doppler sonography to identify feeding arteries associated with parathyroid adenomas. *AJR Am J Roentgenol* 1998; **171**: 819-823 [PMID: 9725323 DOI: 10.2214/ajr.171.3.9725323]
- 14 Kamaya A, Quon A, Jeffrey RB. Sonography of the abnormal parathyroid gland. *Ultrasound Q* 2006; **22**: 253-262 [PMID: 17146333 DOI: 10.1097/01.ruq.0000237260.33509.4f]
- 15 Johnson NA, Yip L, Tublin ME. Cystic parathyroid adenoma: sonographic features and correlation with 99mTc-sestamibi SPECT findings. *AJR Am J Roentgenol* 2010; **195**: 1385-1390 [PMID: 21098199 DOI: 10.2214/AJR.10.4472]
- 16 Chandramohan A, Sathyakumar K, John RA, Manipadam MT, Abraham D, Paul TV, Thomas N, Paul MJ. Atypical ultrasound features of parathyroid tumours may bear a relationship to their clinical and biochemical presentation. *Insights Imaging* 2014; **5**: 103-111 [PMID: 24293304 DOI: 10.1007/s13244-013-0297-x]
- 17 Polga JP, Balikian JP. Partially calcified functioning parathyroid adenoma. Casedemonstrated roentgenographically. *Radiology* 1971; **99**: 55-56 [PMID: 5548688 DOI: 10.1148/99.1.55]
- 18 Randel SB, Gooding GA, Clark OH, Stein RM, Winkler B. Parathyroid variants: US evaluation. *Radiology* 1987; **165**: 191-194 [PMID: 3306784 DOI: 10.1148/radiology.165.1.3306784]
- 19 Vitetta GM, Neri P, Chiecchio A, Carriero A, Cirillo S, Mussetto AB, Codegone A. Role of ultrasonography in the management of patients with primary hyperparathyroidism: retrospective comparison with technetium-99m sestamibi scintigraphy. *J Ultrasound* 2014; **17**: 1-12 [PMID: 24616746 DOI: 10.1007/s40477-014-0067-8]

- 20 **Tsai K**, Liang TZ, Grant EG, Swanson MS, Barnett B. Optimal imaging modality for diagnosis of parathyroid adenoma: Case report and review of the literature. *J Clin Transl Endocrinol Case Rep* 2020; **17**: 100065. [DOI: [10.1016/j.jecr.2020.100065](https://doi.org/10.1016/j.jecr.2020.100065)]
- 21 **Pavlovics S**, Radzina M, Niciporuka R, Ratniece M, Mikelsons M, Tauvena E, Liepa M, Prieditis P, Ozolins A, Gardovskis J, Narbutis Z. Contrast-Enhanced Ultrasound Qualitative and Quantitative Characteristics of Parathyroid Gland Lesions. *Medicina (Kaunas)* 2021; **58** [PMID: [35056309](https://pubmed.ncbi.nlm.nih.gov/35056309/) DOI: [10.3390/medicina58010002](https://doi.org/10.3390/medicina58010002)]
- 22 **Platz Batista da Silva N**, Jung EM, Jung F, Schlitt HJ, Hornung M. VueBox® perfusion analysis of contrast-enhanced ultrasound (CEUS) examinations in patients with primary hyperparathyroidism for preoperative detection of parathyroid gland adenoma. *Clin Hemorheol Microcirc* 2018; **70**: 423-431 [PMID: [30347604](https://pubmed.ncbi.nlm.nih.gov/30347604/) DOI: [10.3233/CH-189307](https://doi.org/10.3233/CH-189307)]
- 23 **Parra Ramírez P**, Santiago Hernando A, Barquiel Alcalá B, Martín Rojas-Marcos P, Lisbona Catalán A, Álvarez Escolá C. Potential Utility of Contrast-Enhanced Ultrasound in the Preoperative Evaluation of Primary Hyperparathyroidism. *J Ultrasound Med* 2019; **38**: 2565-2571 [PMID: [30693978](https://pubmed.ncbi.nlm.nih.gov/30693978/) DOI: [10.1002/jum.14949](https://doi.org/10.1002/jum.14949)]
- 24 **Ling W**, Nie J, Zhang D, Yang Q, Jin H, Ou X, Ma X, Luo Y. Role of Contrast-Enhanced Ultrasound (CEUS) in the Diagnosis of Cervical Lymph Node Metastasis in Nasopharyngeal Carcinoma (NPC) Patients. *Front Oncol* 2020; **10**: 972 [PMID: [32766127](https://pubmed.ncbi.nlm.nih.gov/32766127/) DOI: [10.3389/fonc.2020.00972](https://doi.org/10.3389/fonc.2020.00972)]
- 25 **Chen L**, Chen L, Liu J, Wang B, Zhang H. Value of Qualitative and Quantitative Contrast-Enhanced Ultrasound Analysis in Preoperative Diagnosis of Cervical Lymph Node Metastasis From Papillary Thyroid Carcinoma. *J Ultrasound Med* 2020; **39**: 73-81 [PMID: [31222782](https://pubmed.ncbi.nlm.nih.gov/31222782/) DOI: [10.1002/jum.15074](https://doi.org/10.1002/jum.15074)]
- 26 **Cui XW**, Jenssen C, Saftoiu A, Ignee A, Dietrich CF. New ultrasound techniques for lymph node evaluation. *World J Gastroenterol* 2013; **19**: 4850-4860 [PMID: [23946589](https://pubmed.ncbi.nlm.nih.gov/23946589/) DOI: [10.3748/wjg.v19.i30.4850](https://doi.org/10.3748/wjg.v19.i30.4850)]
- 27 **Azizi G**, Piper K, Keller JM, Mayo ML, Puett D, Earp KM, Malchoff CD. Shear wave elastography and parathyroid adenoma: A new tool for diagnosing parathyroid adenomas. *Eur J Radiol* 2016; **85**: 1586-1593 [PMID: [27501893](https://pubmed.ncbi.nlm.nih.gov/27501893/) DOI: [10.1016/j.ejrad.2016.06.009](https://doi.org/10.1016/j.ejrad.2016.06.009)]
- 28 **Johnson NA**, Tublin ME, Ogilvie JB. Parathyroid imaging: technique and role in the preoperative evaluation of primary hyperparathyroidism. *AJR Am J Roentgenol* 2007; **188**: 1706-1715 [PMID: [17515397](https://pubmed.ncbi.nlm.nih.gov/17515397/) DOI: [10.2214/AJR.06.0938](https://doi.org/10.2214/AJR.06.0938)]
- 29 **Hoang JK**, Sung WK, Bahl M, Phillips CD. How to perform parathyroid 4D CT: tips and traps for technique and interpretation. *Radiology* 2014; **270**: 15-24 [PMID: [24354373](https://pubmed.ncbi.nlm.nih.gov/24354373/) DOI: [10.1148/radiol.13122661](https://doi.org/10.1148/radiol.13122661)]
- 30 **Chazen JL**, Gupta A, Dunning A, Phillips CD. Diagnostic accuracy of 4D-CT for parathyroid adenomas and hyperplasia. *AJNR Am J Neuroradiol* 2012; **33**: 429-433 [PMID: [22135127](https://pubmed.ncbi.nlm.nih.gov/22135127/) DOI: [10.3174/ajnr.A2805](https://doi.org/10.3174/ajnr.A2805)]
- 31 **Gafton AR**, Glastonbury CM, Eastwood JD, Hoang JK. Parathyroid lesions: characterization with dual-phase arterial and venous enhanced CT of the neck. *AJNR Am J Neuroradiol* 2012; **33**: 949-952 [PMID: [22241395](https://pubmed.ncbi.nlm.nih.gov/22241395/) DOI: [10.3174/ajnr.A2885](https://doi.org/10.3174/ajnr.A2885)]
- 32 **Beland MD**, Mayo-Smith WW, Grand DJ, Machan JT, Monchik JM. Dynamic MDCT for localization of occult parathyroid adenomas in 26 patients with primary hyperparathyroidism. *AJR Am J Roentgenol* 2011; **196**: 61-65 [PMID: [21178047](https://pubmed.ncbi.nlm.nih.gov/21178047/) DOI: [10.2214/AJR.10.4459](https://doi.org/10.2214/AJR.10.4459)]
- 33 **Ruda JM**, Hollenbeak CS, Stack BC Jr. A systematic review of the diagnosis and treatment of primary hyperparathyroidism from 1995 to 2003. *Otolaryngol Head Neck Surg* 2005; **132**: 359-372 [PMID: [15746845](https://pubmed.ncbi.nlm.nih.gov/15746845/) DOI: [10.1016/j.otohns.2004.10.005](https://doi.org/10.1016/j.otohns.2004.10.005)]
- 34 **Mahajan A**, Starker LF, Ghita M, Udelsman R, Brink JA, Carling T. Parathyroid four-dimensional computed tomography: evaluation of radiation dose exposure during preoperative localization of parathyroid tumors in primary hyperparathyroidism. *World J Surg* 2012; **36**: 1335-1339 [PMID: [22146947](https://pubmed.ncbi.nlm.nih.gov/22146947/) DOI: [10.1007/s00268-011-1365-3](https://doi.org/10.1007/s00268-011-1365-3)]
- 35 **Grayev AM**, Gentry LR, Hartman MJ, Chen H, Perlman SB, Reeder SB. Presurgical localization of parathyroid adenomas with magnetic resonance imaging at 3.0 T: an adjunct method to supplement traditional imaging. *Ann Surg Oncol* 2012; **19**: 981-989 [PMID: [21879264](https://pubmed.ncbi.nlm.nih.gov/21879264/) DOI: [10.1245/s10434-011-2046-z](https://doi.org/10.1245/s10434-011-2046-z)]
- 36 **Lopez Hänninen E**, Vogl TJ, Steinmüller T, Ricke J, Neuhaus P, Felix R. Preoperative contrast-enhanced MRI of the parathyroid glands in hyperparathyroidism. *Invest Radiol* 2000; **35**: 426-430 [PMID: [10901104](https://pubmed.ncbi.nlm.nih.gov/10901104/) DOI: [10.1097/00004424-200007000-00005](https://doi.org/10.1097/00004424-200007000-00005)]
- 37 **Sacconi B**, Argirò R, Diacinti D, Iannarelli A, Bezzi M, Cipriani C, Pisani D, Cipolla V, De Felice C, Minisola S, Catalano C. MR appearance of parathyroid adenomas at 3 T in patients with primary hyperparathyroidism: what radiologists need to know for pre-operative localization. *Eur Radiol* 2016; **26**: 664-673 [PMID: [26024849](https://pubmed.ncbi.nlm.nih.gov/26024849/) DOI: [10.1007/s00330-015-3854-5](https://doi.org/10.1007/s00330-015-3854-5)]
- 38 **Yildiz S**, Aralasmak A, Yetis H, Kilicarslan R, Sharifov R, Alkan A, Toprak H. MRI findings and utility of DWI in the evaluation of solid parathyroid lesions. *Radiol Med* 2019; **124**: 360-367 [PMID: [30607865](https://pubmed.ncbi.nlm.nih.gov/30607865/) DOI: [10.1007/s11547-018-0970-8](https://doi.org/10.1007/s11547-018-0970-8)]
- 39 **Merchavy S**, Luckman J, Guindy M, Segev Y, Khaffif A. 4D MRI for the Localization of Parathyroid Adenoma: A Novel Method in Evolution. *Otolaryngol Head Neck Surg* 2016; **154**: 446-448 [PMID: [26598499](https://pubmed.ncbi.nlm.nih.gov/26598499/) DOI: [10.1177/0194599815618199](https://doi.org/10.1177/0194599815618199)]
- 40 **Murugan N**, Kandasamy D, Sharma R, Goyal A, Gupta AK, Tandon N, Gupta N, Goswami R, Vurthaluru S, Damle N, Agrawal S. Comparison of 4DMRI and 4DCT for the preoperative evaluation of patients with primary hyperparathyroidism. *Eur J Radiol* 2021; **138**: 109625 [PMID: [33714845](https://pubmed.ncbi.nlm.nih.gov/33714845/) DOI: [10.1016/j.ejrad.2021.109625](https://doi.org/10.1016/j.ejrad.2021.109625)]
- 41 **Vallabhajosula S**. (18)F-labeled positron emission tomographic radiopharmaceuticals in oncology: an overview of radiochemistry and mechanisms of tumor localization. *Semin Nucl Med* 2007; **37**: 400-419 [PMID: [17920348](https://pubmed.ncbi.nlm.nih.gov/17920348/) DOI: [10.1053/j.semnuclmed.2007.08.004](https://doi.org/10.1053/j.semnuclmed.2007.08.004)]
- 42 **Ishizuka T**, Kajita K, Kamikubo K, Komaki T, Miura K, Nagao S, Nozawa Y. Phospholipid/Ca²⁺-dependent protein kinase activity in human parathyroid adenoma. *Endocrinol Jpn* 1987; **34**: 965-968 [PMID: [3450512](https://pubmed.ncbi.nlm.nih.gov/3450512/) DOI: [10.1507/endoerj1954.34.965](https://doi.org/10.1507/endoerj1954.34.965)]
- 43 **Tay D**, Das JP, Yeh R. Preoperative Localization for Primary Hyperparathyroidism: A Clinical Review. *Biomedicines* 2021; **9** [PMID: [33917470](https://pubmed.ncbi.nlm.nih.gov/33917470/) DOI: [10.3390/biomedicines9040390](https://doi.org/10.3390/biomedicines9040390)]
- 44 **Parvinian A**, Martin-Macintosh EL, Goenka AH, Durski JM, Mullan BP, Kemp BJ, Johnson GB. (11)C-Choline PET/CT for Detection and Localization of Parathyroid Adenomas. *AJR Am J Roentgenol* 2018; **210**: 418-422 [PMID: [29140118](https://pubmed.ncbi.nlm.nih.gov/29140118/) DOI: [10.2214/AJR.17.18312](https://doi.org/10.2214/AJR.17.18312)]

- 45 **Michaud L**, Burgess A, Huchet V, Lefèvre M, Tassart M, Ohnona J, Kerrou K, Balogova S, Talbot JN, Périé S. Is 18F-fluorocholine-positron emission tomography/computerized tomography a new imaging tool for detecting hyperfunctioning parathyroid glands in primary or secondary hyperparathyroidism? *J Clin Endocrinol Metab* 2014; **99**: 4531-4536 [PMID: 25215560 DOI: 10.1210/jc.2014-2821]
- 46 **Kluijfhout WP**, Vorselaars WM, Vriens MR, Borel Rinkes IH, Valk GD, de Keizer B. Enabling minimal invasive parathyroidectomy for patients with primary hyperparathyroidism using Tc-99m-sestamibi SPECT-CT, ultrasound and first results of (18)F-fluorocholine PET-CT. *Eur J Radiol* 2015; **84**: 1745-1751 [PMID: 26047823 DOI: 10.1016/j.ejrad.2015.05.024]



Published by **Baishideng Publishing Group Inc**
7041 Koll Center Parkway, Suite 160, Pleasanton, CA 94566, USA
Telephone: +1-925-3991568
E-mail: bpgoffice@wjgnet.com
Help Desk: <https://www.f6publishing.com/helpdesk>
<https://www.wjgnet.com>

